

# Effect mechanism of unfrozen water on the frozen soil-structure interface during the freezing-thawing process

Liyun Tang<sup>\*1</sup>, Yang Du<sup>§1</sup>, Lang Liu<sup>2,3</sup>, Long Jin<sup>4</sup>, Liujun Yang<sup>1</sup> and Guoyu Li<sup>\*\*5</sup>

<sup>1</sup>Architecture and Civil Engineering School, Xi'an University of Science and Technology, Xi'an, China

<sup>2</sup>Energy School, Xi'an University of Science and Technology, Xi'an 710054, China

<sup>3</sup>Key Laboratory of Western Mine Exploitation and Hazard Prevention with Ministry of Education, Xi'an University of Science and Technology, Shaanxi, Xi'an 710054, China

<sup>4</sup>CCCC First Highway Consultants Co. Ltd. Shaanxi, Xi'an 710000, China

<sup>5</sup>State Key Laboratory of Frozen Soil Engineering,

Cold and Arid Regions Environmental and Engineering Research Institute, Chinese Academy of Sciences

(Received January 23, 2020, Revised July 3, 2020, Accepted July 6, 2020)

**Abstract.** The interaction between the frozen soil and building structures deteriorates with the increasing temperature. A nuclear magnetic resonance (NMR) stratification test was conducted with respect to the unfrozen water content on the interface and a shear test was conducted on the frozen soil-structure interface to explore the shear characteristics of the frozen soil-structure interface and its failure mechanism during the thawing process. The test results showed that the unfrozen water at the interface during the thawing process can be clearly distributed in three stages, i.e., freezing, phase transition, and thawing, and that the shear strength of the interface decreases as the unfrozen water content increases. The internal friction angle and cohesive force display a change law of "as one falls, the other rises," and the minimum internal friction angle and maximum cohesive force can be observed at -1 °C. In addition, the change characteristics of the interface strength parameters during the freezing process were compared, and the differences between the interface shear characteristics and failure mechanisms during the frozen soil-structure interface freezing-thawing process were discussed. The shear strength parameters of the interface was subjected to different changes during the freezing-thawing process because of the different interaction mechanisms of the molecular structures of ice and water in case of the ice-water phase transition of the test sample during the freezing-thawing process.

**Keywords:** frozen soil-structure interface; freezing-thawing; NMR; unfrozen water content

## 1. Introduction

The soil-structure interface is weak, and the failure of this interface can result in the destruction of building structures (Fatahi *et al.* 2014, Ngo *et al.* 2019). Additionally, this interface is an important medium for the mutual transmission of stress and deformation between soil and the structures. The increased global temperatures and climate change amplification in cold regions have considerably changed the mechanical properties of the frozen soil-structure interface (Shiklomanov *et al.* 2017, Xu *et al.* 2020), considerably affecting the bearing capacity of the interface and the structural stability (Wang *et al.* 2018, 2019, 2019). The degraded frozen soil-structure interaction induced by thawing can be mainly attributed to the changes in soil properties and the decreased foundation-bearing capacity during the thawing process, both of which result in uneven settlement and even instability of the structure

(Lyazgin *et al.* 2004, Niu *et al.* 2011, Tang *et al.* 2019). The degradation of the mechanical properties of the frozen soil-structure interface during the thawing process has become a leading basic scientific problem that should be solved based on the rapid development of engineering construction in cold regions.

An ice film forms on the interface when the temperature between the frozen soil and the structure decreases because of the difference in thermal conductivity between the two materials (Sayles *et al.* 1987), which is responsible for the freezing strength of the interface (Nixon *et al.* 2011, Rist *et al.* 2012, Wen *et al.* 2016). Lee *et al.* (2013) systematically improved the normal-temperature soil direct shear test apparatus and placed it in a walk-in low-temperature environment box. Further, an aluminum plate was used to simulate the contact surface of the structure, and the freezing strength of the interface between the frozen soil and contact surface was tested under different freezing temperatures and normal stress conditions. Wen *et al.* (2016) conducted a direct shear test on the frozen soil-concrete interface and observed that the freezing strength between the soil and structure gradually increased as the temperature decreased. In addition, the increased normal pressure can not only increase the freezing strength but also the water content's influence on shear strength. Thus, the effect of freezing strength decreases with the increasing water content in a sample and normal pressure. Liu *et al.*

\*Corresponding author, Ph.D.

E-mail: tangly@xust.edu.cn

\*\*Corresponding author, Ph.D.

E-mail: guoyuli@lzb.ac.cn

§Contributed equally as the first author

conducted direct shear (Liu *et al.* 2014a) and dynamic direct shear (Liu *et al.* 2014b) tests on the frozen soil-structure interfaces during the freezing process. They observed that the frozen soil-structure interface's freezing strength includes the freezing force of ice at the interface and the cohesion of the soil particles and concrete surface. Thus, the peak strength of the interface will increase with the decreasing temperature. Shi *et al.* (2016) conducted a shear test on the artificial frozen sand-structure interface during the freezing process. They observed that the unfrozen water near the interface gradually decreased with the increasing temperature of the interface. Thus, the cementation of the interface increased, increasing the freezing strength limit of the interface and growth rate as the temperature decreased. During the freezing process, the freezing strength gradually increased between the soil and the structure as the temperature decreased and the unfrozen water at the frozen soil-structure interface gradually transformed into ice. In contrast, the ice crystals at the interface melted into unfrozen water during the thawing process, and the freezing strength gradually decreased. Wang *et al.* (2017) obtained the interface strength during the thawing process based on a direct shear test of the interface between the thawing soil and a structure. Thus, the temperature is an important factor affecting the soil-structure interaction, which can be attributed to the change in the presence of water at the interface, i.e., the change in temperature alters the ice (unfrozen water) content at the interface. Therefore, the variations in unfrozen water content at the frozen soil-structure interface must be understood to explore the mechanical characteristics of the interface. Since Tsytoovich (1960) proposed the concept of unfrozen water content in frozen soil, testing this property has been one of the main difficulties in the field of frozen soil. However, the recent introduction of various new tests in the field has provided improved methods to measure the unfrozen water content at the soil-structure interface. For example, the nuclear magnetic resonance (NMR) testing technology provides a direct and non-destructive unfrozen water testing method. NMR is not considerably affected by external interference during water distribution measurements. Further, NMR does not disturb the sample and exhibits a short single-test time and high accuracy (Mohnke *et al.* 2002, Zhou *et al.* 2015, Li *et al.* 2016).

Therefore, this study explores the variation of unfrozen water content with respect to the shearing characteristics of the frozen soil-structure during the thawing process. In addition, shear tests were conducted on the frozen soil-structure samples using laboratory simulation tests. NMR delamination testing was used for the first time to test the samples thawed to different temperatures within 10 mm of the interface. The variations in the shear strength and unfrozen water content were used to analyze the mechanical properties of the interface. Thus, the variations in the unfrozen water content, internal friction angle, and cohesive force during the thawing process were obtained with the degree of thawing. Further, the mechanical properties of the frozen soil-structure interface during the freezing-thawing process were discussed and analyzed based on the results of the shear tests with respect to the frozen soil-structure interface obtained previously. This also revealed the frozen soil-structure interface interaction mechanism during the freezing-thawing process to provide a theoretical reference

for establishing a systematic freezing-thawing damage model and various engineering applications.

## 2. Test design

### 2.1 Test materials and sample preparation

The test soil was silty clay, which is a typical soil type in the Qinghai-Tibet permafrost region. The soil was dried, crushed, sieved, and remolded based on the "Standard for Soil Test Method"(GB/T50123). The plastic limit, liquid limit, and plasticity index of the test soil were 14.6%, 30.8%, and 16.3, respectively. The soil samples with a unified water content of 20% were remolded to obtain a dry sample density of 1.7 g/cm<sup>3</sup>. All the parameters of the concrete prepared in this study were in accordance with the actual application parameters used in engineering in frozen soil regions to better reflect the contact status of the frozen soil-structure interface in actual engineering. Table 1 presents the parameters of the cast-in-place concrete, and Fig. 1 shows the grain-size grading curve of the soil particles.

Table 1 Parameters of the cast-in-place concrete

Water-cement ratio	Ratio of cement to aggregate	Ratio of cement to antifreeze	Cement label	Grain-size grading (mm)		
				0-2	2-5	5-10
0.5	1:3	1:0.15	P.O 42.5	31%	56%	13%

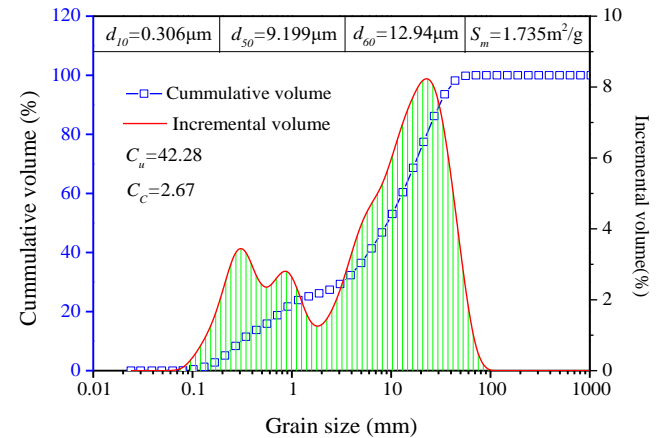


Fig. 1 The soil-particle grain-size grading curve

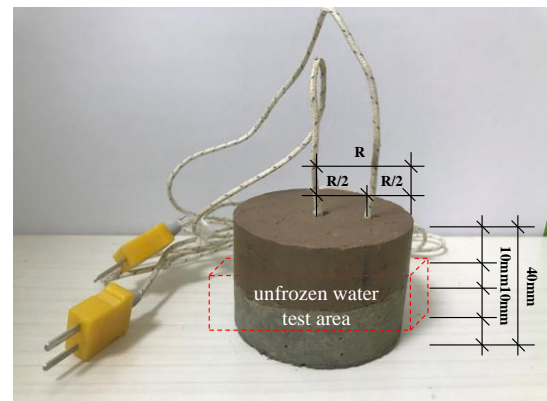


Fig. 2 Frozen soil-structure interface sample

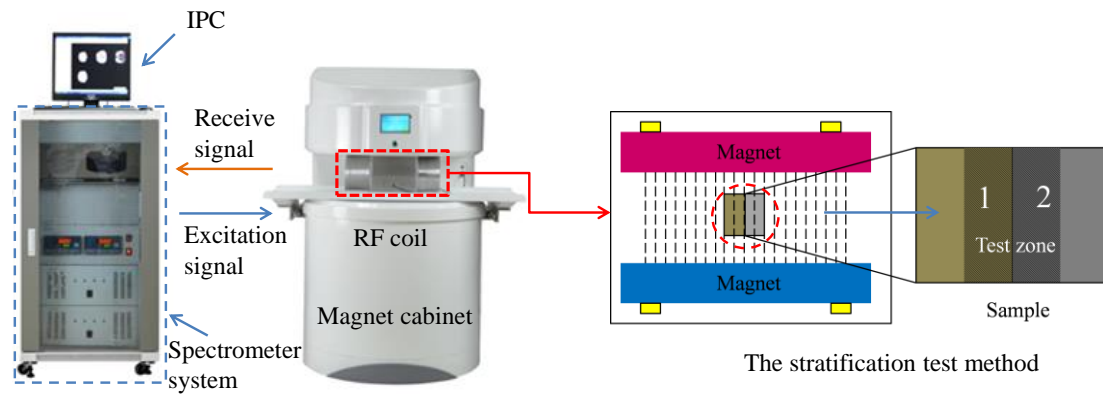


Fig. 3 NMR stratified test

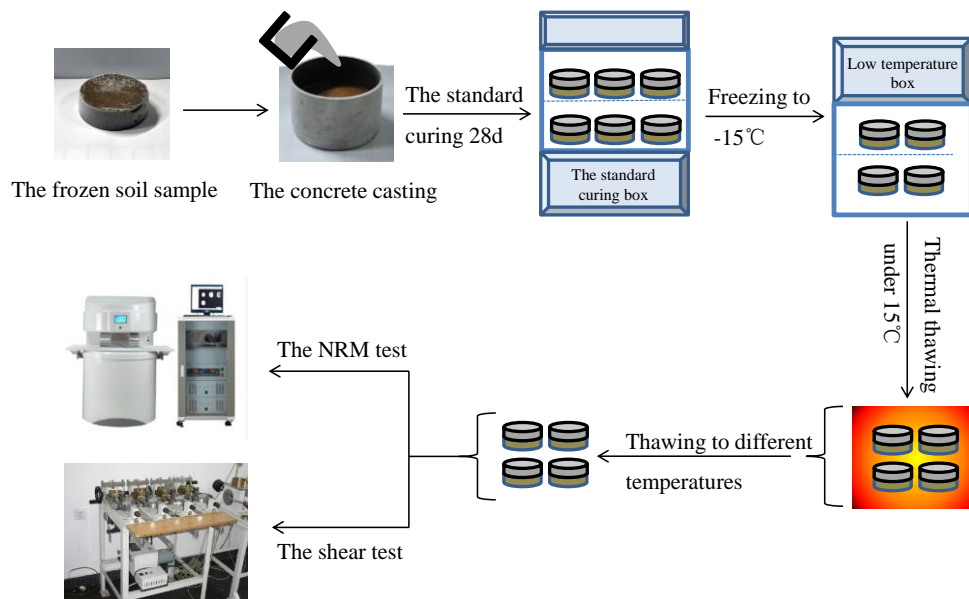


Fig. 4 Test procedure design

The interface samples were prepared in accordance with the “Standard for Soil Test Method” (GB/T50123) for obtaining ring-cutting soil samples with dimensions of 61.8 mm × 20 mm. A hydraulic jack was used to transfer the 20-mm-high ring-cutting soil sample to a high sample ring cutter with dimensions of 61.8 mm × 40 mm. The high sample ring cutter containing the 20 mm soil sample was subsequently placed in a low-constant-temperature test box and frozen at  $-15^{\circ}\text{C}$  for 12 h. After the frozen high sample ring cutter was removed, the evenly mixed concrete was cast into the high sample ring cutter, removed after freezing, and fully vibrated to ensure that the cast-in-place concrete was in complete contact with the surface of the frozen soil sample and that concrete was sufficiently compacted. After concrete casting, the interface samples were cured for 28 days (temperature difference =  $\pm 1^{\circ}\text{C}$ ) at an external ambient temperature of  $5^{\circ}\text{C}$ , which sample preparation refers to the cast-in-place concrete–frozen soil preparation process (Du *et al.* 2019). After curing the sample for 28 days, it was moved to the low-constant-temperature test box for freezing to achieve a sample-freezing temperature of  $-15^{\circ}\text{C}$ . Simultaneously, a temperature sensor embedded in the

interface was used to facilitate real-time temperature monitoring at the sample interface. TP-K01 thermocouple temperature sensors with an accuracy of  $0.1^{\circ}\text{C}$  were used during the test, and two probes were embedded at the center and  $1/2R$  of each sample. The temperature difference between the two probes was  $0^{\circ}\text{C}$ – $0.12^{\circ}\text{C}$ . The temperatures at the sample center and  $1/2R$  were averaged to obtain the average interface temperature. Fig. 2 shows the frozen soil-structure interface sample and temperature probe arrangement.

## 2.2 NMR unfrozen water test principle and methods

The MacroMR12-150H-I NMR tester, which was jointly developed and produced by the Chinese Academy of Sciences and Suzhou Newmai Co., Ltd., was selected for conducting the test. The NMR tester comprises four main parts, i.e., an industrial computer (including a spectrometer system), a radio frequency (RF) unit, a magnet cabinet, and a temperature control system.

The built-in phase stratification test method (the built-in SE\_SPI sequence) was adopted as the stratified T2

relaxation (transverse relaxation time) test, as shown in Fig. 3. The NMR testing principle for measuring the unfrozen water content is to establish a relation between the unfrozen water content and temperature by detecting the variation of the echo signal intensity (T2 spectrum) with temperature. The area enclosed by the T2 distribution curve is proportional to the number of hydrogen atoms in the fluid within the detection range; this value is directly proportional to the water content (Du *et al.* 2019, Tice *et al.* 1981). The unfrozen water content testing method used in this study was based on this technique. Fig. 3 shows the principle of the stratified test method at the interface. The RF instrument range was 200 mm and was divided into 20 layers of 10 mm each. The sample was placed at the RF center axis, and the shaded part of the sample in the figure was the signal section required for the test. The sum of the T2 spectrum areas of the two layers (1, 2) was the signal value of the hydrogen atoms in the liquid water at the interface.

### 2.3 Test plan

First, the interface sample frozen to  $-15^{\circ}\text{C}$  was placed in an environment with a temperature of  $15^{\circ}\text{C}$ . Subsequently, the sample was thawed naturally through thermal convection with the air. In this test, the HT-9815 four-channel temperature sensor was embedded at the interface for real-time monitoring of the temperature change during the thawing process.

Then, the NMR stratification test method was used for monitoring the nuclear magnetic signal of the sample interface during the thawing process. The magnet's constant temperature system and RF unit power were turned on in advance to ensure NMR magnetic field stability and uniformity when the sample was being tested at different temperatures. Further, the acquisition parameters were set when the temperature of the area to be tested and the test temperature were identical and the NMR signal did not exhibit any further changes. A Fourier transform inversion software was used to obtain the T2 distribution, and the nuclear magnetic signal data were saved. The relation between the temperature and unfrozen water content of the interface sample during the thawing process was obtained based on the unfrozen water content of the interface at different temperatures with respect to the NMR signal strength.

Finally, a direct shear test was conducted. The interface shear test was conducted in a low-temperature laboratory to ensure that the external environment did not affect the temperature during the shearing process. A strain-controlled direct shear tester produced by the Nanjing Soil Research Instrument Factory was used to conduct the shear test of the frozen soil-cast-in-place concrete interface. Shear tests were conducted on the samples thawed to  $-15^{\circ}\text{C}$  (the shear test failed at this temperature),  $-10^{\circ}\text{C}$ ,  $-7^{\circ}\text{C}$ ,  $-5^{\circ}\text{C}$ ,  $-3^{\circ}\text{C}$ ,  $-1^{\circ}\text{C}$ ,  $0^{\circ}\text{C}$ ,  $1^{\circ}\text{C}$ ,  $5^{\circ}\text{C}$ , and  $10^{\circ}\text{C}$ . The shear box was cooled to reduce its temperature before each shear test, ensuring that its temperature is reduced to a value consistent with the temperature of the sample; thus, the sample temperature error during the shear process could be decreased. The shear stresses at the time of failure were obtained for a cutting

speed of  $0.8\text{ mm}\cdot\text{min}^{-1}$  and normal pressures of 50, 100, 200, and 300 kPa. Further, the roughness of the concrete test block was tested after the shearing test, and the average roughness was observed to be 2.3 mm. The shear strength parameters of the interface were determined based on the Coulomb formula. Fig. 4 presents the test procedure design.

## 3. Results

### 3.1 Change law of unfrozen water content at the interface during the thawing process

Fig. 5 shows the temperature-unfrozen water content change curve of the frozen soil-structure interface during the thawing process. In this figure, the sample's curve shows a three-stage distribution during thawing, i.e., a freezing stage, a phase transition stage, and a thawing stage. Based on the temperature-unfrozen water content change law, a T2 spectrogram was obtained when the sample was thawed to  $-10^{\circ}\text{C}$ ,  $-1^{\circ}\text{C}$ , and  $10^{\circ}\text{C}$ . The x-axis in Fig. 5 indicates the T2 relaxation time, whereas the y-axis indicates the NMR signal value.

The area of the NMR T2 spectrum is positively correlated with the unfrozen water content. Therefore, large T2 spectral area indicates large unfrozen water content. In Fig. 5, the peak value of the NMR signal increases, and the T2 spectrum shifts to the right during the thawing process. An increase in peak value indicates an increase in NMR signal strength at the same T2 relaxation. Thus, the amount of thawed ice in pores having the same size increases. In contrast, a rightward shift indicates a gradual increase in unfrozen water content in large pores. Fig. 5 shows that the area of the T2 spectrum is small and that the peak signal is low; the unfrozen water content at the interface mainly exists in small pores at  $-10^{\circ}\text{C}$ . The area of the T2 spectrum increased clearly when the sample temperature increased from  $-10^{\circ}\text{C}$  to  $-1^{\circ}\text{C}$ , and the signal peak value increased significantly. Further, the peak gradually shifted rightward. In addition, the second peak point of the T2 spectrum could be observed at  $-1^{\circ}\text{C}$ , indicating that the ice crystals in the large pores at the interface began to melt gradually. The

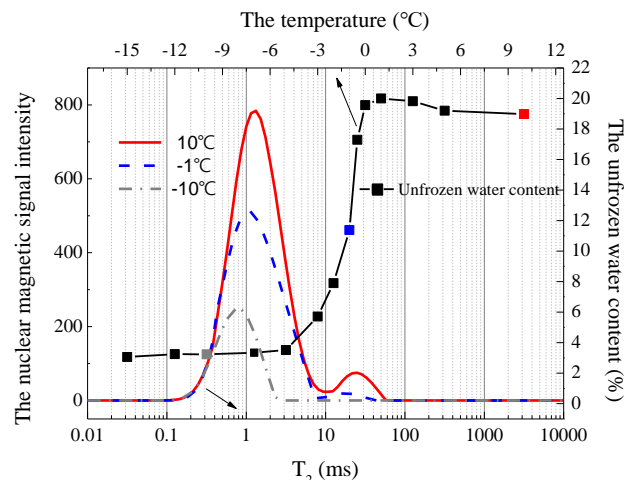


Fig. 5 Unfrozen water and T2 spectrogram at the interface

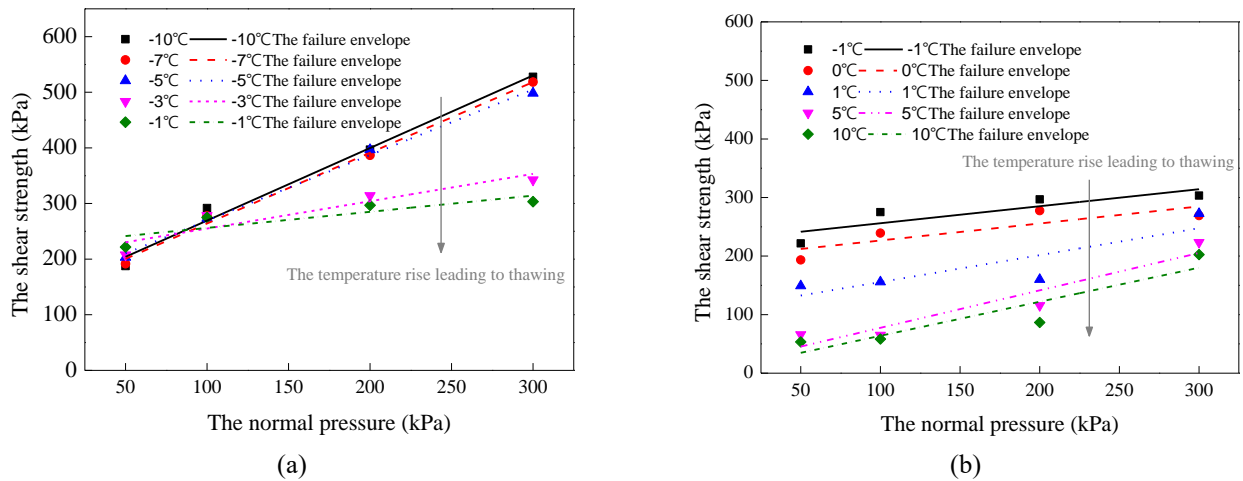


Fig. 6 Shear failure envelope diagram under different thawing temperatures and normal pressures

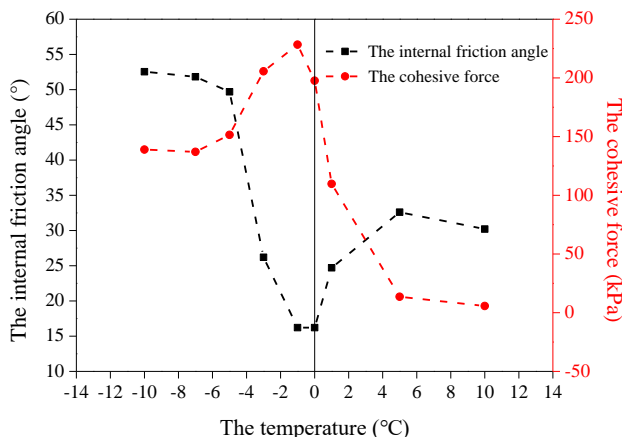


Fig. 7 Change law chart of the shear strength parameters at different temperatures

area and value of the second peak continued to increase with the sample temperature. The internal ice completely melted when the sample was fully thawed; however, the interface temperature-unfrozen water content curve shows that the sample temperature continued to increase when the unfrozen water content reached its peak. The unfrozen water content at the interface decreased slightly. This may be because of the creation of a water potential difference when the soil water migrated to the interface during the freezing process and the unfrozen water migrated from the interface into the soil during the thawing process.

### 3.2 Change law of the interface shear strength during the thawing process

Fig. 6 denotes the shear failure envelope observed when the frozen soil-structure interface sample was thawed at different temperatures. The shear strength of the sample increases with the increasing normal pressure when the sample was thawed at different temperatures, and the increased amplitude is related to the thawing temperature. In addition, the interface’s shear strength gradually decreases during the thawing process. In Fig. 6(a), the sample temperature is still negative. At this time, the

interface’s shear strength significantly increases with the increasing normal pressure. However, the temperature of the sample increases as the thawing process continues, and the influence of the increase in normal pressure on the shear strength of the interface gradually decreases. Fig. 6(b) shows the situation when the sample was thawed at a positive temperature. The slope of the failure envelope varies less under different temperatures as the sample temperature increases and increases slightly toward the end of the thawing process. Thus, the influence of the increase in normal pressure on the sample shear strength gradually decreases and tends to be gentle when thawed to a positive temperature.

The shear strength of frozen soil-structure interface (Figs. 6(a) and 6(b)) gradually decreases throughout the thawing process. The decrease in shear strength can be mainly attributed to the decrease in the internal friction angle of the interface during the initial stage of thawing. Further thawing increased the sample temperature. Meanwhile, the decrease in cohesive force at the interface gradually reduced the interface shear strength, and the internal friction at the interface tended to be stable.

### 3.3 Change law of the shear strength parameters during the thawing process

Fig. 7 depicts the change law of the frozen soil–structure interface’s shear strength parameters with the increasing thawing degree of the sample. Thus, the internal friction angle and cohesive force of the interface show a change behavior of “as one falls, the other rises” during the thawing process. The internal friction angle of the sample interface decreased slightly during the initial thawing stage, and the increase in cohesive force was also observed to be small. When the sample temperature increased to  $-5^{\circ}\text{C}$  and continued to thaw, the internal friction angle of the interface rapidly decreased and became minimum at  $-1^{\circ}\text{C}$ . Subsequently, the cohesive force of the interfaces gradually increased to reach its peak value at  $-1^{\circ}\text{C}$ ; however, this rate of increase is significantly less than the rate of decrease with respect to the internal friction angle. The cohesive force decreased significantly as the test sample continued to

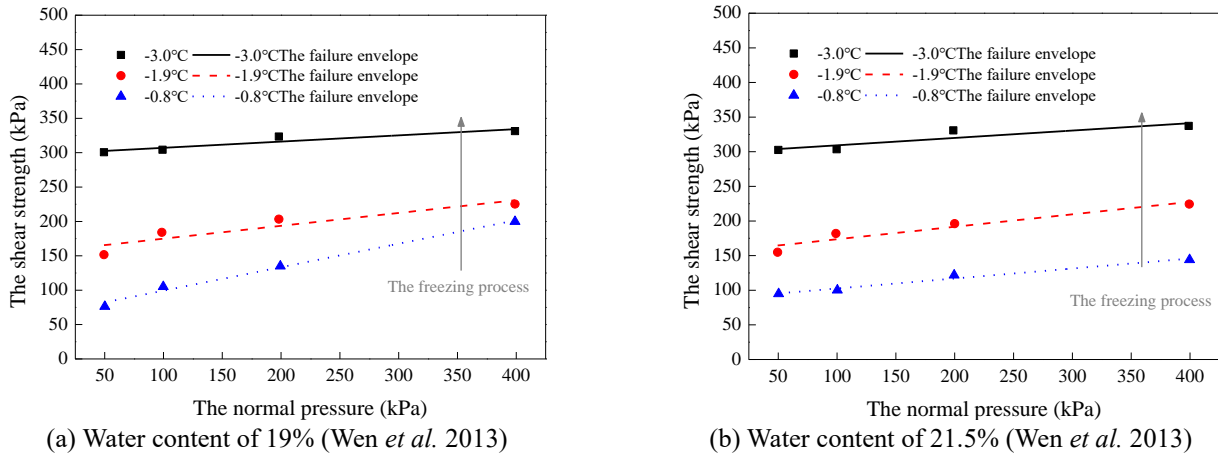


Fig. 8 The shear failure envelope diagram at different temperatures and normal pressures

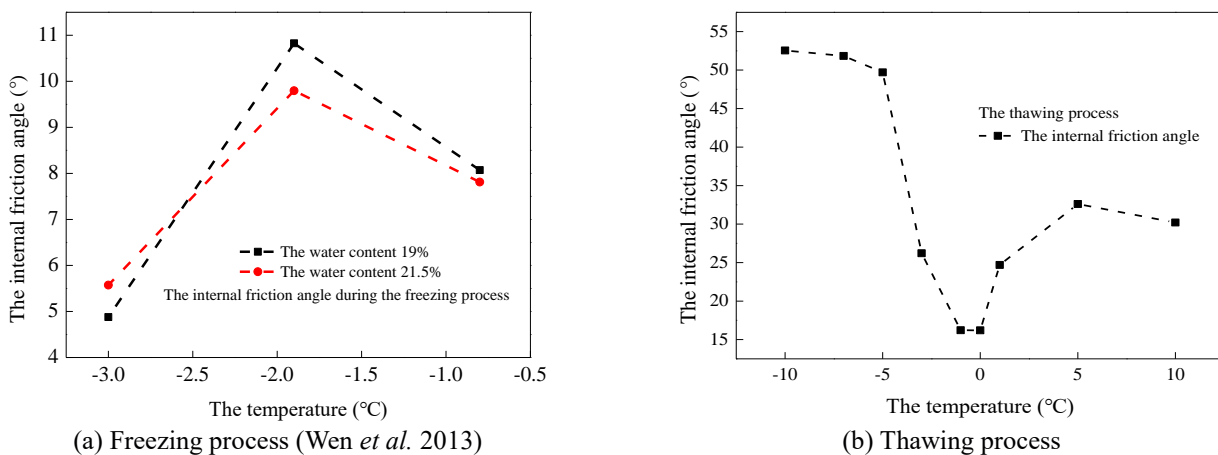


Fig. 9 Friction-angle changes in case of the frozen and melted interfaces

thaw after  $-1^{\circ}\text{C}$ , whereas the internal friction angle only increased slightly. However, its increase rate was significantly lower than the decrease rate of the cohesive force. Then, the thawing of the sample entered the positive-temperature section. The test sample was fully thawed, and the internal friction angle and cohesive force of the interface were observed to be stable. Regardless, when compared with the initial stage of thawing, the internal friction angle and cohesive force of the frozen soil-structure interface considerably declined after the thawing process.

#### 4. Discussion

##### 4.1 Analysis of the interface shear strength during the freezing process

We explored the interaction differential characteristic of the frozen soil-structure interface during the freezing-thawing process by comparing and analyzing the results obtained by Wen *et al.* (2013) through frozen soil-concrete interface shear tests to understand the shear characteristics of the frozen soil-structure interface.

A frozen soil-concrete sample in previously studied Wen *et al.* (2013) had a diameter of 61.8 mm and a height of 40 mm. These dimensions are identical to those of the sample

considered in this study. The dry density of the sample was  $1.68\text{ g/cm}^3$  Wen *et al.* (2013), and the direct shear test was an unconsolidated and undrained fast shear test, which uses sample parameters and shearing methods similar to those adopted in this study. Therefore, this study was compared with that conducted by Wen *et al.* (2013) using water contents of 19% and 21.5%. Fig. 8(a) shows the shear failure envelope of the frozen soil-structure test sample during the freezing process of Wen *et al.* (2013) in the temperature section from  $-0.8^{\circ}\text{C}$  to  $-3^{\circ}\text{C}$ . By comparing the failure envelope in Fig. 8(a) with that in Fig. 8(b), which shows the corresponding temperature section of the thawing process in this study, the shear strength of the frozen soil-structure interface is observed to increase as the temperature decreases during the freezing process. Subsequently, it decreases gradually with the increasing temperature during the thawing process.

##### 4.2 Comparison and analysis of the internal friction angle of the freezing-thawing interface

Fig. 9 denotes the change curve of the internal friction angles at the frozen soil-structure interface during the freezing-thawing process. The shear strength of the interface increases when the water content of the test sample is 19% and 21.5%. All the internal friction angles initially increase and subsequently decrease within the

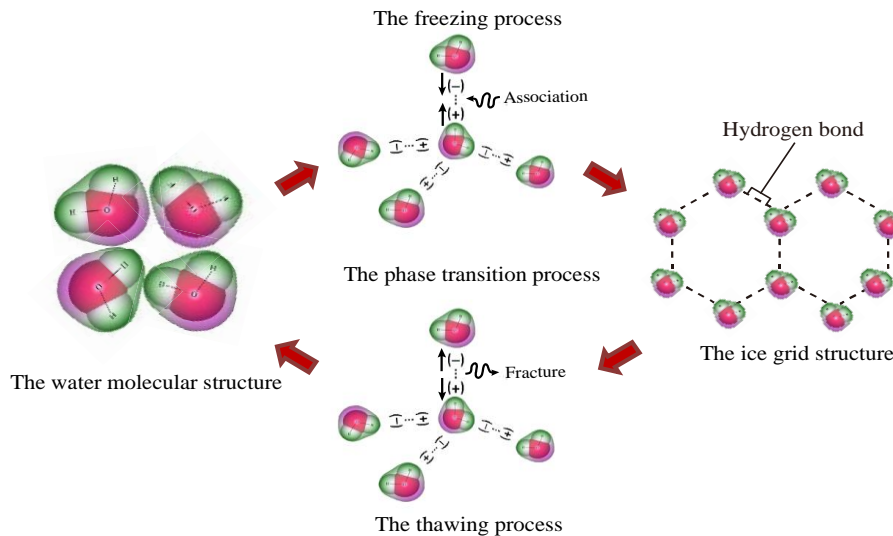


Fig. 10 The phase transition mechanism of water molecules during freezing–thawing process

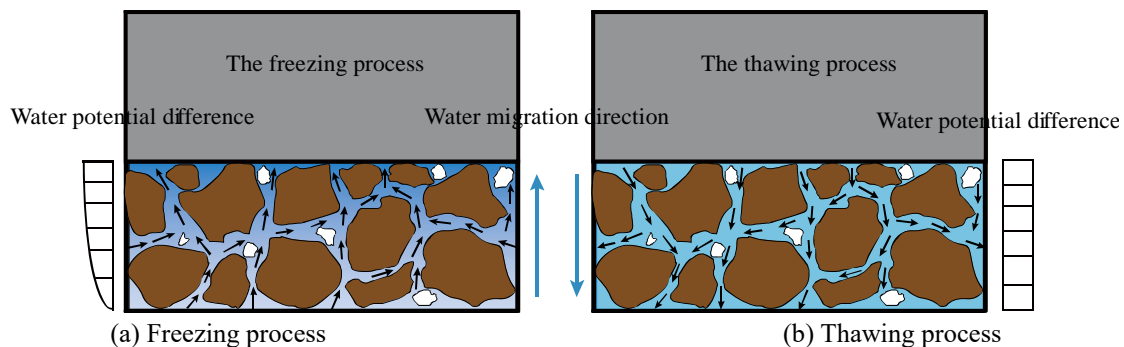


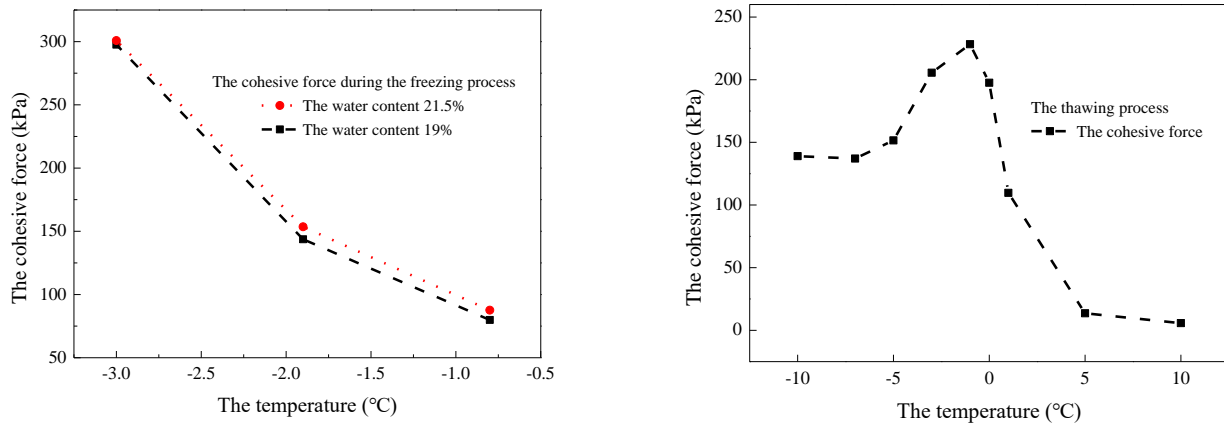
Fig. 11 The water migration diagram of the freezing–thawing process

freezing temperature range specified by Wen *et al.* (2013), and the peak value could be observed when the test sample was frozen to  $-1.9^{\circ}\text{C}$ . Extreme internal friction angles could be observed at different temperatures during the freezing–thawing process. Such angles could be observed at a lower temperature during the freezing process than that in the thawing process. Thus, the extreme internal friction angle could be observed earlier during the thawing process than that during the freezing process at the same temperature. This can be attributed to the unfrozen water content of the test sample during the freezing–thawing process (Kruse *et al.* 2017, Tan *et al.* 2015), denoting that the unfrozen water content at the interface is an important factor affecting mechanical properties.

Fig. 9 denotes two different change laws with respect to the internal friction angle between the frozen soil–structure interfaces during the freezing–thawing process. During the freezing process, the internal friction angle initially increased and subsequently decreased; however, the internal friction angle initially decreased and subsequently increased with the increasing thawing degree during the thawing process. This is closely related to the changes in unfrozen water content at the interface during the phase transition stage and the conversion mechanism between the ice and water test samples during the freezing–thawing process. Because of the differences in thermal conductivity between the soil and structure, an ice film gradually formed at the

frozen soil–structure interface during the freezing process (Spaans and Baker 1996). In addition, the free water in the test sample transformed into ice, and the internal friction angle of the interface initially increased and subsequently decreased because of changes in the molecular structure of water during the freezing process

As shown in Fig. 10, the water molecules were circular, loose, and irregular in fluid state, and extremely small frictional resistance could be observed between the molecules during the frozen–structure shearing process. During the freezing process, the water molecules connected via hydrogen bonds to form ice molecules with a spatial four-sided conical structure, resulting in large intermolecular resistance between the molecules during sliding. The connection between the ice molecules became increasingly stable with the continuously decreasing temperature, and a spatial hexahedral grid structure was gradually formed. Therefore, during the initial freezing stage, water transformed into ice crystals and the internal friction angle of the frozen soil–structure interface increased. The internal friction angle further decreased as the freezing process continued because soil and concrete exhibit different thermal conductivities. During the freezing process, the soil water migrated to the interface and accumulated to gradually form an ice film, reducing the effective contact area between the soil and the structure. The internal friction angle of the interface

(a) Freezing process (Wen *et al.* 2013)

(b) Thawing process

Fig. 12 The change curve of the cohesive force of the freezing-thawing interfaces

initially decreased and subsequently increased during the thawing process because the hydrogen bonds between the ice molecules break with the thawing of ice crystals, resulting in the gradual change of the ordered ice molecules into a loose and disordered form, i.e., water. Therefore, the internal friction angle of the interface gradually decreased during the thawing process. However, because of water migration during the freezing process, a water potential difference could be observed inside the soil, as shown in Fig. 11(a), and the ice film at the thawing interface was gradually thawed to produce a water film. Subsequently, the water potential difference between the interface and the inside of the soil began to change (Auriault *et al.* 1985), and the interface water migrated to the inside of the soil according to Darcy's law (Terzaghi *et al.* 1996, You *et al.* 2017), as shown in Fig. 11(b). Furthermore, the soil permeability coefficient gradually increases with the increase in temperature (Nishimura and Wang 2018, Xu *et al.* 2020); thus, the seepage velocity gradually increases. The effective contact area of the corresponding soil-structure increases with the decreasing water film, causing the internal friction angle to recover. The internal friction angle gradually decreases with the redistribution of the soil water and eventually stabilizes.

#### 4.3 Comparative analysis of the cohesive force of the freezing-thawing interfaces

The cohesive force on the soil-structure interface was partially provided by the adsorption force of the water between the interfaces of the soil-structure surface particles. Fig. 12(a) shows that the cohesive force between the frozen soil-structure interfaces increased as the temperature decreased during the freezing process, which can be attributed to the migration of free water to the water-rich zone at the interface during the freezing process. Further, the adsorption force between the interface and the soil particles increased. In addition, when the temperature decreased, the water in the test sample froze to become ice, and an ice bonding force was observed at the interface and between the soil particles. The aforementioned phenomena are the main reasons for the increased cohesive force at the

frozen soil-structure interface during the freezing process.

As shown in Fig. 12(b), the cohesive force of the frozen soil-structure interface increases during initial thawing, possibly because of the gradual thawing of ice between the frozen soil and structure, the unfrozen water content increases, and the adsorption force of interface and between the soil particles increases. Here, the ice bonding force decreased because of ice thawing. However, the bonding force was generally high because less ice was thawed during the initial thawing stage. With the increasing thawing depth, the ice-rich zone gradually became a water-rich zone, resulting in the depletion of the ice bonding force. The internal water migrated again under the action of the water potential difference. Furthermore, the migration of free water could be repeatedly observed in the sample, and the initial bond deterioration could be observed at the interface and between the soil particles. Additionally, many pores and micro-cracks were formed in the original water-rich zone of the interface, decreasing the cohesive force of the interface during the later thawing stage. When the internal water field of the test sample was redistributed, the water potential difference gradually recovered and the cohesive force of the frozen soil-structure interface gradually stabilized.

#### 5. Limitations of the study and future research

In this study, the change law with respect to the unfrozen water content and shear strength at the frozen soil-structure interface is developed based on previous studies in case of the thawing process using the NMR stratification testing technology. Therefore, this study was more innovative than the existing research. However, there was a lack of in-depth analysis about the interaction mechanisms of the frozen soil-structure interfaces during the thawing process. For example, the volume change and water redistribution within a certain range of the interface during the freezing-thawing process will change the internal microstructure of the soil, affecting the interaction between the frozen soil and the structure. In this study, the failure mechanism at the frozen soil-structure interface during the

thawing process was only analyzed based on the unfrozen water content changes at the interface and the resulting changes in mechanical properties. However, the intuitive and quantitative microscopic experimental studies were insufficient. For example, it was unclear whether the bond formed between the soil particles changed or was destroyed during the thawing process, whether the soil particle group changed shape, or whether the change in the internal microstructure of the soil during the thawing process can increase the range of the soil shearing displacement zone. Therefore, further microscopic experiments should be conducted to study the frozen soil-structure interaction mechanisms during the thawing process. In addition, any study and analysis should be quantitative and refined to understand the failure mechanism of the frozen soil-structure interface during the thawing process.

## 6. Conclusions

To explore the change law of unfrozen water content and shear strength of the frozen soil-structure interface during the thawing process, the NMR method was used for stratification testing of the unfrozen water content and the interface shear test was applied. The intrinsic relation between the change in unfrozen water content and interface shear strength during the thawing process was also ascertained. When combined with the results obtained from previous studies about the frozen soil-structure interface freezing process, the following conclusions were obtained.

- During the thawing process of the frozen soil-structure sample, the unfrozen water content at the interface exhibited an obvious three-stage distribution, including the freezing, phase transition, and thawing stages. Further, water migration could be observed during the entire thawing process, with free water migrating from the interface into the soil.

- The shear strength between the frozen soil and the structure gradually decreased during the freezing-thawing process. This decrease was mainly caused by the decrease in the internal friction angle of the interface during the initial stage of the thawing process. Further, the test sample increased with the increasing thawing degree. In this case, the gradually decreasing cohesive force at the interface became the main cause for the decreasing shear strength of the interface.

- The internal friction angle and cohesive force of the frozen soil-structure interface exhibited a change law of “as one falls, the other rises” during the thawing process. The minimum internal friction angle and maximum cohesive force could be observed at  $-1^{\circ}\text{C}$ .

- The strength parameters of the frozen soil and structure changed differently during the freezing-thawing process. The internal friction angles of the interface exhibited opposite characteristics during the freezing-thawing process because of changes in the molecular structure of water when it froze during phase transition.

- The change law with respect to the cohesive force during the freezing process is incomplete, and the extreme value point cannot be observed, which can be attributed to the narrow test temperature range ( $-0.8^{\circ}\text{C}\sim-3^{\circ}\text{C}$ ) and the

change law having not been fully presented. Therefore, increasing the temperature range of the freezing process and clarifying the change law with respect to the cohesive force during the freezing process are crucial for studying the frozen soil-structure interaction during the freezing-thawing process.

## Acknowledgments

This research was supported by the National Natural Science Foundation of China (No. 41502298).

## Conflict of interest

The authors declare no conflict of interest concerning the publication of this paper.

## References

- Auriault, J.L., Borne, L. and Chambon, R. (1985), “Dynamics of porous saturated media, checking of the generalized law of Darcy”, *J. Acoust. Soc. Amer.*, **77**(5), 1641-1650.  
<https://doi.org/10.1121/1.391962>.
- Du, Y., Tang, L., Yang, L., Wang, X. and Bai, M. (2019), “Interface characteristics of frozen soil-structure thawing process based on nuclear magnetic resonance”, *Chin. J. Geotech. Eng.*, **41**(12), 2316-2322.  
<https://doi.org/10.11779/CJGE201912017>.
- Fatahi, B., Tabatabaiefar, S. and Samali, B. (2014), “Soil-structure interaction vs site effect for seismic design of tall buildings on soft soil”, *Geomech. Eng.*, **6**(3), 293-320.  
<https://doi.org/10.12989/gae.2014.6.3.293>.
- Kruse, A.M., Darrow, M.M. and Akagawa, S. (2017), “Improvements in measuring unfrozen water in frozen soils using the pulsed nuclear magnetic resonance method”, *J. Cold Reg. Eng.*, **32**(1), 04017016.  
[https://doi.org/10.1061/\(ASCE\)CR.1943-5495.0000141](https://doi.org/10.1061/(ASCE)CR.1943-5495.0000141).
- Lee, J., Kim, Y. and Choi, C. (2013), “A study for adfreeze bond strength developed between weathered granite soils and aluminum plate”, *J. Korean Geoenviron. Soc.*, **14**(12), 23-30.  
<https://doi.org/10.14481/jkges.2013.14.12.023>.
- Li, J.L., Zhou, K.P., Liu, W.J. and Deng, H.W. (2016), “NMR research on deterioration characteristics of microscopic structure of sandstones in freeze-thaw cycles”, *T. Nonferr. Metal. Soc. China*, **26**(11), 2997-3003.  
[https://doi.org/10.1016/S1003-6326\(16\)64430-8](https://doi.org/10.1016/S1003-6326(16)64430-8).
- Liu, J.K., Cui, Y.H., Wang, P.C. and Lv, P. (2014), “Design and validation of a new dynamic direct shear apparatus for frozen soil”, *Cold Reg. Sci. Technol.*, **106**, 207-215.  
<https://doi.org/10.1016/j.coldregions.2014.07.010>.
- Liu, J.K., Lv, P., Cui, Y.H. and Liu, J.Y. (2014), “Experimental study on direct shear behavior of frozen soil-concrete interface”, *Cold Reg. Sci. Technol.*, **104**, 1-6.  
<https://doi.org/10.1016/j.coldregions.2014.04.007>.
- Lyazgin, A.L., Lyashenko, V.S., Ostroborodov, S.V., Ol'shanskii, V.G., Bayasan, R.M., Shevtsov, K.P. and Pustovoit, G.P. (2004), “Experience in the prevention of frost heave of pile foundations of transmission towers under northern conditions”, *Power Technol. Eng.*, **38**(2), 124-126.  
<https://doi.org/10.1023/B:HYCO.0000036365.64731.4c>.
- Mohnke, O. and Yaramanci, U. (2002), “Smooth and block inversion of surface NMR amplitudes and decay times using

- simulated annealing”, *J. Appl. Geophys.*, **50**(1-2), 163-177.  
[https://doi.org/10.1016/S0926-9851\(02\)00137-4](https://doi.org/10.1016/S0926-9851(02)00137-4).
- Ngo, V.L., Kim, J.M. and Lee, C. (2019), “Influence of structure-soil-structure interaction on foundation behavior for two adjacent structures: Geo-centrifuge experiment”, *Geomech. Eng.*, **19**(5), 407-420.  
<https://doi.org/10.12989/gae.2019.19.5.407>.
- Nishimura, S. and Wang, J. (2018), “A simple framework for describing strength of saturated frozen soils as multi-phase coupled system”, *Géotechnique*, **69**(8), 659-671.  
<https://doi.org/10.1680/jgeot.17.P.104>.
- Niu, F.J., Ma, W. and Wu, Q.B. (2011), “Thermal stability of roadbeds of the Qinghai-Tibet railway in permafrost regions and the main freezing-thawing hazards”, *J. Earth Sci. Environ.*, **33**(2), 196-206.  
<https://doi.org/10.3969/j.issn.1672-6561.2011.02.016>.
- Nixon, J.F. and Morgenstern, N.R. (2011), “Thaw-consolidation tests on undisturbed fine-grained permafrost”, *Can. Geotech. J.*, **11**(1), 202-214. <https://doi.org/10.1139/t74-012>.
- Pan, D., Li, S., Xu, Z., Zhang, Y., Lin, P. and Li, H. (2019), “A deterministic-stochastic identification and modelling method of discrete fracture networks using laser scanning: Development and case study”, *Eng. Geol.*, **262**, 105310.  
<https://doi.org/10.1016/j.enggeo.2019.105310>.
- Rist, A., Phillips, M. and Springman, S.M. (2012), “Inclinable shear box simulations of deepening active layers on perennially frozen scree slopes”, *Permafrost Periglac.*, **23**(1), 26-38.  
<https://doi.org/10.1002/ppp.1730>.
- Sayles, F.H., Baker, T.H.W., Gallavres, F., Jessberger, H.L., Kinoshita, S., Sadovskiy, A.V. and Vyalov, S.S. (1987), “Classification and laboratory testing of artificially frozen ground”, *J. Cold Reg. Eng.*, **1**(1), 22-48.  
[https://doi.org/10.1061/\(asce\)0887-381x\(1987\)1:1\(22\)](https://doi.org/10.1061/(asce)0887-381x(1987)1:1(22)).
- Shi, Q.B., Yang, P. and Wang, G.L. (2016), “Experimental study on adfreezing strength of the interface between artificial frozen sand and structure”, *Chin. J. Rock Mech. Eng.*, **35**(10), 2142-2151. <https://doi.org/10.13722/j.cnki.jrme.2015.1511>.
- Shiklomanov, N.I., Streletskiy, D.A., Swales, T.B. and Kokorev, V.A. (2017), “Climate change and stability of urban infrastructure in Russian permafrost regions: Prognostic assessment based on GCM climate projections”, *Geograph. Rev.*, **107**(1), 125-142. <https://doi.org/10.1111/gere.12214>.
- Spaans, E.J. and Baker, J.M. (1996), “The soil freezing characteristic: Its measurement and similarity to the soil moisture characteristic”, *Soil Sci. Soc. Amer. J.*, **60**(1), 13-19.  
<https://doi.org/10.2136/sssaj1996.03615995006000010005x>.
- Tan, L., Wei, C.F., Tian, H.H., Zhou, J.Z. and Wei, H.Z. (2015), “Experimental study of unfrozen water content of frozen soils by low-field nuclear magnetic resonance”, *Rock Soil Mech.*, **36**(6), 1566-1572. <https://doi.org/10.16285/j.rsm.2015.06.006>.
- Tang, L., Wang, K., Deng, L., Yang, G., Chen, J. and Jin, L. (2019), “Axial loading behaviour of laboratory concrete piles subjected to a resistivity model for testing unfrozen water content of frozen soil/permafrost degradation”, *Cold Reg. Sci. Technol.*, **166**, 102820.  
<https://doi.org/10.1016/j.coldregions.2019.102820>.
- Terzaghi, K., Peck, R.B. and Mesri, G. (1996), *Soil Mechanics in Engineering Practice*, John Wiley and Sons.
- The National Standards Compilation Group of the People’s Republic of China (1999), *GB/T50123—1999 Standard for Soil Test Method*, China Planning Press, Beijing, China.
- Tice, A.R., Anderson, D.M. and Sterrett, K.F. (1981), “Unfrozen water contents of submarine permafrost determined by nuclear magnetic resonance”, *Eng. Geol.*, **18**(1-4), 135-146.  
<https://doi.org/10.1016/B978-0-444-42010-7.50017-7>.
- Tsyrovich, N.A. (1960), “Problems of frozen soil mechanics in engineering practice”, Highway Res Board Special Report, (60).
- Wang, B., Liu, Z.Q., Zhao, X.D., Zhi, L. and Xiao, H.H. (2017), “Experimental study on shearing mechanical characteristics of thawing soil and structure interface under high pressure”, *Rock Soil Mech.*, **38**(12), 3540-3546.
- Wang, F., Li, G., Ma, W., Wu, Q., Serban, M., Vera, S., Alexandr, F., Jiang, N. and Wang, B. (2019), “Pipeline-permafrost interaction monitoring system along the China-Russia crude oil pipeline”, *Eng. Geol.*, **254**, 113-125.  
<https://doi.org/10.1016/j.enggeo.2019.03.013>.
- Wang, S., Wang, Q., Qi, J. and Liu, F. (2018), “Experimental study on freezing point of saline soft clay after freeze-thaw cycling”, *Geomech. Eng.*, **15**(4), 997-1004  
<https://doi.org/10.12989/gae.2018.15.4.997>.
- Wang, X., Li, S., Xu, Z., Hu, J., Pan, D. and Xue, Y. (2019), “Risk assessment of water inrush in karst tunnels excavation based on normal cloud model”, *Bull. Eng. Geol. Environ.*, **78**(5), 3783-3798. <https://doi.org/10.1007/s10064-018-1294-6>.
- Wen, Z., Yu, H.H., Zhang, J.M., Dong, S.S., Ma, W., Niu, F.J., Zhao, S.P. and Yang, Z. (2013), “Experimental study on adfreezing bond strength of interface between silt and foundation of Qinghai-Tibetan transmission line”, *Chin. J. Geotech. Eng.*, **35**(12), 2262-2267.
- Wen, Z., Yu, Q., Ma, W., Dong, S., Wang, D., Niu, F. and Zhang, M. (2016), “Experimental investigation on the effect of fiberglass reinforced plastic cover on adfreeze bond strength”, *Cold Reg. Sci. Technol.*, **131**, 108-115.  
<https://doi.org/10.1016/j.coldregions.2016.07.009>.
- Xu, Z., Lin, P., Xing, H. and Wang, J. (2020), “Mathematical modelling of cumulative erosion ratio for suffusion in soils”, *Proc. Inst. Civ. Eng. Geotech. Eng.*, 1-11.  
<https://doi.org/10.1680/jgeen.19.00082>.
- Xu, Z.H., Huang, X., Li, S.C., Lin, P., Shi, X.S. and Wu, J. (2020), “A new slice-based method for calculating the minimum safe thickness for a filled-type karst cave”, *Bull. Eng. Geol. Environ.*, **79**(2), 1097-1111.  
<https://doi.org/10.1007/s10064-019-01609-9>.
- You, Y., Wang, J., Wu, Q., Yu, Q., Pan, X., Wang, X. and Guo, L. (2017), “Causes of pile foundation failure in permafrost regions: The case study of a dry bridge of the Qinghai-Tibet Railway”, *Eng. Geol.*, **230**, 95-103.  
<https://doi.org/10.1016/j.enggeo.2017.10.004>.
- Zhou, K.P., Bin, L.I., Li, J.L., Deng, H.W. and Feng, B.I.N. (2015), “Microscopic damage and dynamic mechanical properties of rock under freeze-thaw environment”, *T. Nonferr. Metal. Soc. China*, **25**(4), 1254-1261.  
[https://doi.org/10.1016/S1003-6326\(15\)63723-2](https://doi.org/10.1016/S1003-6326(15)63723-2).

GC